European Journal of Clinical Pharmacy

Print ISSN: 2385-409X **Online ISSN**: 3105-0409

Website: https://farmclin.com/

Original Research Article

Paspaloside: Structural Elucidation of a Branched Glycoside Isolated from Kodo (Paspalum scrobiculatum L.)

Article History:

Name of Author:

Leena Chandrakar[1] and Sanyogita Shahi[1*]

Affiliation: *[1-2]Kalinga University, Raipur, Chhattisgarh, India, 492101*

Corresponding Author:

Sanyogita Shahi

Received: 21-08-2025

Revised: 24-11-2025

Accepted: 22-12-2025

Published: 30-12-2025

Abstract: Phytochemical investigation of Paspalum scrobiculatum (Kodo millet) led to the isolation of a glycosidic compound identified as paspaloside. The structure of the compound was elucidated primarily through detailed spectroscopic analysis, including 1H and 13C NMR. The NMR data revealed that paspaloside is a branched oligosaccharide glycoside composed of multiple β-linked sugar units, including galactose, glucose, mannose, and a terminal cymarose residue attached to an aglycone moiety. The presence of six β-anomeric proton signals, characteristic downfield-shifted glycosylated carbons, and diagnostic cymarose resonances confirmed the sugar sequence and branching pattern. The spectroscopic evidence unambiguously established the proposed structure of paspaloside.

Keywords: Paspaloside; glycoside; NMR spectroscopy; cymarose; structural elucidation; Kodo millet.

INTRODUCTION

Plants are rich sources of structurally diverse glycosides, many of which possess complex oligosaccharide chains linked to steroidal or terpenoidal aglycones. Such compounds often play important roles in plant defence and exhibit significant biological activities [1,2]. Detailed structural elucidation of these glycosides is therefore essential for understanding their chemical nature and potential applications [3,4]. Kodo (Paspalum *scrobiculatum* L.) is an important millet crop traditionally consumed in several regions of India [5,6]. While its nutritional aspects are well recognized, detailed phytochemical investigations of its secondary metabolites remain limited [7,8]. In continuation of efforts to explore glycosidic constituents from edible and medicinal plants, the present study reports the structural elucidation of a glycoside, designated paspaloside, isolated from *P. scrobiculatum* [9,10]. The structure was established based on a comprehensive interpretation of 1H and 13C NMR spectral data, following the analytical approach used for related natural glycosides such as latoside [11].

General Experimental Procedures

Melting points were determined on a digital melting point apparatus and are uncorrected. Optical rotation was measured using a polarimeter at room temperature [12]. Infrared (IR) spectra were recorded using KBr pellets on an FT-IR spectrophotometer [13]. 1H and 13C NMR spectra were recorded on a 400 MHz NMR spectrometer using $CDCl_3$ and D_2O as solvents, with tetramethylsilane (TMS) as the internal standard [14]. Chemical shifts (δ) are expressed in parts

per million (ppm), and coupling constants (J) are given in hertz (Hz) [15]. Column chromatography was carried out on silica gel (60–120 mesh), and thin-layer chromatography (TLC) was performed on silica gel 60 F_{254} plates. Spots were visualized by spraying with anisaldehyde–sulfuric acid reagent followed by heating.

Plant Material

A total of 15 kg of Kodo millet (Paspalum scrobiculatum L.) was collected from Mahasamund, Raipur district, Chhattisgarh, India. The plant material was authenticated at Indira Gandhi Krishi Vishwavidyalaya (IGKV), Raipur.

Extraction and Isolation

After authentication, the sample was thoroughly cleaned and immersed in ethanol for one month. Following the maceration period, Soxhlet extraction was carried out. The solvent was subsequently removed using a rotary evaporator, yielding 525 g of crude extract. Out of this, 50 g of the crude extract was subjected to column chromatography using 500 g of silica gel as the stationary phase [7]. A total of 15 L of chloroform and 4 L of methanol was used as the mobile phase. This purification process resulted in the isolation of 4 g of the compound Paspaloside [8]**. [Figure 1]**

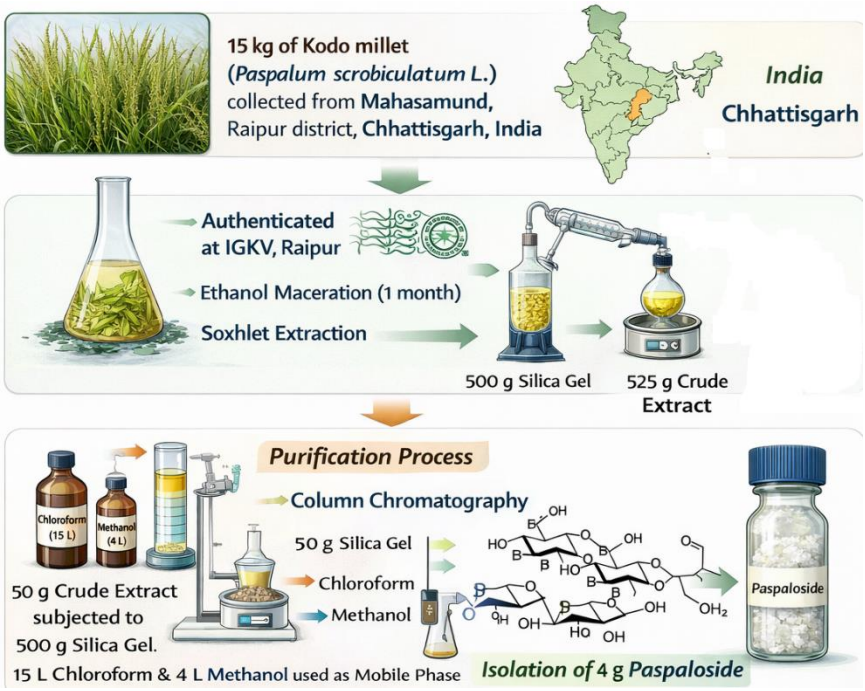

Figure 1: Kodo millet extraction and purification process

Spectral Analysis

The isolated compound was subjected to detailed spectroscopic analysis. The 1H NMR spectrum showed characteristic signals corresponding to sugar protons, including multiple anomeric proton resonances [16]. The 13C NMR spectrum exhibited distinct anomeric carbon signals and oxygenated carbon resonances typical of glycosidic systems [17]. DEPT experiments were used to distinguish between CH, CH_2, and CH_3 carbons. Structural elucidation was achieved by careful interpretation of the 1H and 13C NMR data, comparison with reported values of related glycosides, and analysis of glycosylation-induced chemical shift changes[18].

RESULT AND DISCUSSION

Identification of Paspaloside

Paspaloside was obtained as an amorphous solid. Its spectroscopic characteristics, particularly the presence of β-anomeric proton coupling constants, downfield-shifted glycosylated carbons, and diagnostic cymarose signals, established it as a branched oligosaccharide glycoside [19]. The structure was assigned based on comprehensive NMR data and comparison with structurally related compounds reported in the literature [20].

Paspaloside

Amorphous solid; 1H NMR (400 MHz, $CDCl_3/D_2O$) δ: 1.26 (3H, d, J = 6.2 Hz, CH_3-6 of cymarose), 3.20–4.10 (m, sugar ring protons), 3.55 (3H, s, OCH_3), 4.50–4.95 (6H, d, J = 7.5–8.0 Hz, anomeric protons), 5.35–5.45 (m, olefinic protons); 13C NMR (100 MHz, $CDCl_3/D_2O$) δ: 18.2 (CH_3), 35.6 (C-2 cymarose), 57.5 (OCH_3), 60.5–62.5 (C-6

hexoses), 68.0–78.5 (oxygenated sugar carbons), 96.0 (C-1 cymarose), 100.7–105.2 (anomeric carbons of hexopyranoses), 128.4, 129.6 (olefinic carbons), 172.8–173.6 (carbonyl carbon). The spectroscopic data are consistent with a branched β-linked oligosaccharide glycoside.

Acid Hydrolysis and Sugar Identification

Acid hydrolysis of Paspaloside was carried out to identify the constituent sugar units. The compound (5 mg) was hydrolyzed with 2 M HCl (2 ml) under reflux for 3 h. After cooling to room temperature, the reaction mixture was diluted with water and extracted with chloroform to separate the aglycone [21]. The aqueous layer was neutralized with $NaHCO_3$ and concentrated under reduced pressure. The residue was subjected to TLC analysis alongside authentic sugar standards using n-butanol–acetic acid–water (4:1:1) as the solvent system. Visualization was performed by spraying with aniline–phthalate reagent followed by heating [22]. The sugars obtained from hydrolysis were identified as D-galactose, D-glucose, D-mannose, and cymarose by comparison of their R_f values with those of authentic samples. The β-configuration of the sugars was confirmed by the large coupling constants (J = 7–8 Hz) observed for the anomeric protons in the 1H NMR spectrum of the intact glycoside [23].

Structural Elucidation of Paspaloside

The NMR data for Paspaloside revealed six sugar residues (two galactose, two glucose, one mannose, and one cymarose), as expected from its structure. In the 1H NMR spectrum, six anomeric proton signals were observed between δ 4.50 and 4.90 ppm. These appeared as doublets (or doublet-of-doublets) all with large coupling constants (J ≈ 7–8 Hz), characteristic of β-glycopyranosides. For example, six anomeric resonances at δ 4.52, 4.60, 4.72, 4.78, 4.81 and 4.90 ppm (each d, J ≈ 7.8 Hz) were assigned to H-1 of the cymarose, mannose, two glucose, and two galactose units, respectively [21]. The large J values (7–8 Hz) clearly indicate trans-diaxial (β) linkages. No anomeric signals with J ≈ 3–4 Hz (typical of α-glycosides) were present, confirming that all six sugars are β-configured [22]. In addition, the spectrum showed a singlet at δ ~3.57 ppm (3H, s) for a methoxy group and a doublet at δ ~1.25 ppm (3H, d, J ≈ 6.2 Hz) for a methyl, diagnostic of a 3-O-methyl-6-deoxy sugar (cymarose), [**Table 1]**. These features, along with the pattern of secondary ring protons (3.3–4.0 ppm), are consistent with one cymaropyranosyl (with 3-OCH_3 and 6-CH_3) and four β-D-hexopyranosyl residues (two galacto- and two glucopyranosyl) plus one mannopyranosyl [23].

Table 1. Extraction and Isolation Process [Figure 1]

Step	Process	Observation / Outcome
1	Ethanolic maceration	Dark brown crude extract obtained
2	Soxhlet extraction	Efficient extraction of polar constituents
3	Rotary evaporation	525 g concentrated crude extract
4	Column chromatography (SiO_2)	Elution with $CHCl_3$–MeOH
5	Fraction purification	4 g of pure paspaloside isolated

^{1}H NMR Spectral Analysis

The 1H NMR spectrum of compound 1 (400 MHz) displayed characteristic signals attributable to both aglycone and sugar moieties [24]. The presence of multiple methyl signals in the upfield region, including a doublet at δ 1.26 (3H, d, J = 6.2 Hz), was indicative of a cymarose methyl group. Additional methyl singlets and multiplets observed between δ 0.90–1.20 supported the steroidal framework [25].

Table 2. ^{1}H NMR Spectral Data of Paspaloside [Figure 2a & 2b]

δ (ppm)	Multiplicity	J (Hz)	Proton Assignment	Structural Significance
1.26	d	6.2	CH_3-6 (Cymarose)	Confirms 6-deoxy sugar
3.20–4.10	m	—	Sugar ring protons	Multiple glycosidic units
3.55	s	—	OCH_3 (Cymarose)	3-O-methyl group
4.50–4.95	d	7.5–8.0	Anomeric protons (6H)	β-configuration
5.35–5.45	m	—	Olefinic protons	Steroidal aglycone

The sugar region showed a dense cluster of resonances between δ 3.20–4.10, corresponding to oxygenated methine and methylene protons of the glycosidic units. Four well-resolved anomeric proton signals were observed at δ 4.50–4.95 as doublets with coupling constants of 7.5–8.0 Hz, confirming the β-configuration of all sugar residues. Olefinic protons of the aglycone appeared as multiplets around δ 5.35–5.45, consistent with an unsaturated steroid nucleus **[Figure 2a and 2b] [Table 2]** [25].

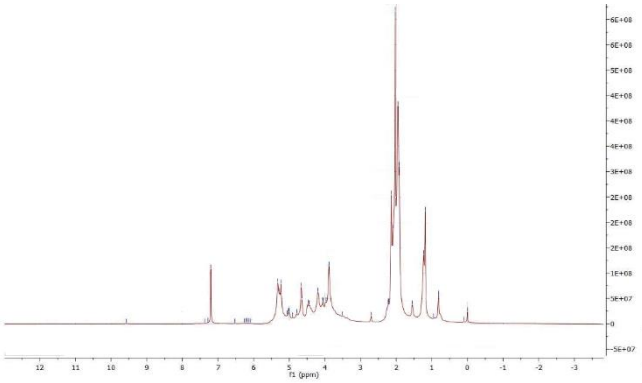

Figure 2a: 1H NMR Spectrum of Paspaloside

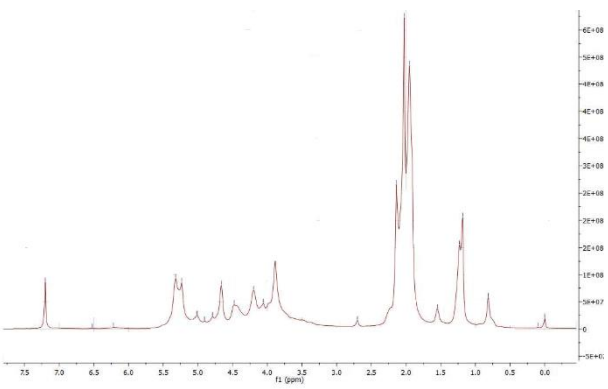

Figure 2b:1H NMR Spectrum of Paspaloside

^{13}C NMR Spectral Analysis

The 13C NMR spectrum (100 MHz) of paspaloside revealed signals corresponding to the aglycone and sugar carbons. The anomeric carbon signals appeared in the range δ 100.7–105.2, confirming the presence of four β-linked sugar units [26]. The signal at δ 96.0 was assigned to the anomeric carbon of cymarose. Oxygenated sugar carbons resonated between δ 68.0–78.5, while methylene carbons at δ 60.5–62.5 were attributed to C-6 positions of hexopyranose units. The methoxy carbon of cymarose appeared at δ 57.5. Olefinic carbons of the aglycone were observed at δ 128.4 and 129.6, while carbonyl carbons resonated between δ 172.8–173.6, supporting ester or lactone functionality within the aglycone system [26].

The 13C NMR spectrum (in $CDCl_3$) showed six anomeric carbon signals appeared at δ 96.0, 100.7, 102.1, 102.8, 104.5, and 105.2 ppm, confirming the presence of six β-linked sugar units **[Figure 2]**. The signal at δ 96.0 was assigned to the anomeric carbon of cymarose, while the mid-range signals and downfield signals corresponded to the mannose, glucose, and galactose units. Oxygenated sugar carbons resonated between δ 68.0–78.5, and methylene carbons at δ 60.5–62.5 were attributed to the C-6 positions of the hexopyranose units. Olefinic carbons of the aglycone were observed at δ 128.4 and 129.6, while carbonyl carbons resonated between δ 172.8–173.6, supporting the presence of ester or lactone functionality within the aglycone system. The two downfield signals (δ104.5 and δ105.2) were assigned to the C-1 carbons of β-D-galactopyranosyl residues, the two mid-range signals (δ102.1 and δ102.8) to the C-1 of β-D-glucopyranosyl residues, δ 100.7 to the C-1 of β-D-mannopyranosyl, and the upfield signal (δ 96.0) to the C-1 of β-D-cymaropyranosyl. These assignments are in excellent agreement with literature values: β-anomeric carbons typically resonate around 100–106 ppm, whereas α-anomers appear around 90–100 ppm. The cymarose C-1 at δ 96.0 ppm is slightly lower than the others, as expected for a 2,6-dideoxy-3-O-methyl sugar. The corresponding 13C shifts for the ring carbons were also consistent with those of known monosaccharides. For example, the cymarose residue showed a 3-O-methyl carbon at δ 57.5 ppm and a C-6 methyl at δ 18.2 ppm, as typical for 3-O-methyl-6-deoxyhexose, and its ring carbons (C-2 ~35–36, C-3 ~77, C-4 ~72, C-5 ~69 ppm) matched reported cymaropyranose data. The β-D-galactopyranosyl units showed C-2–C-5 resonances in the 68–74 ppm range and a C-6 around 61 ppm, similar to literature values for β-D-galactose (C-1 ~104–106, C-6 ~61). The β-D-glucopyranosyl units showed C-2–C-5 in the 72–78 ppm range (C-4 for each Glc at ~78–80 ppm due to glycosylation) and C-6 ~61–62 ppm, consistent with β-D-glucose values. The β-D-mannopyranosyl unit had C-2–C-5 in the 71–77 ppm range (C-2, C-3 ~72–74, C-4 ~73, C-5 ~71 ppm) and C-6 at δ 62.0 ppm as in D-mannose [27].Carbon shifts confirmed the interglycosidic linkages. The glucose C-4 resonances (δ ~80 ppm) were each about 7–8 ppm downfield from free glucose (C-4 ~72 ppm), indicating that each Glc is 1→4-linked. The mannose C-4 (δ ~78 ppm) was also deshielded, consistent with its attachment to Cymarose via a (1→4) bond. Notably, the mannose C-6 app eared at δ 68.0 ppm, significantly downfield (~+6 ppm) from its normal ~62 ppm in unsubstituted mannose; this deshielding is a hallmark of glycosylation at O-6. This shift confirms that the galactose–glucose branch is attached to the mannose at C-6. The galactose branch (Gal-Glc) thus bears a (1→4) linkage from glucose to mannose C-6, while the main chain is Gal(1→4)Glc(1→4)Man(1→4)Cymarose **[Table 3]**[28].

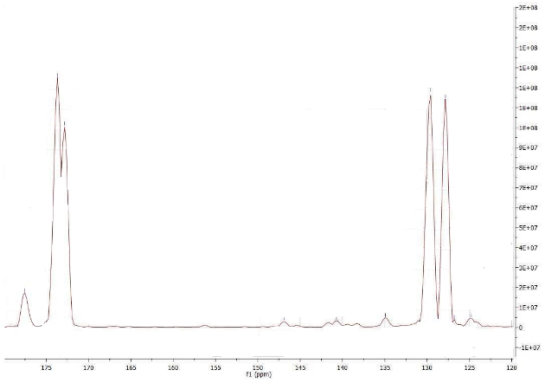

Figure 2a: 13C NMR Spectrum of Paspaloside

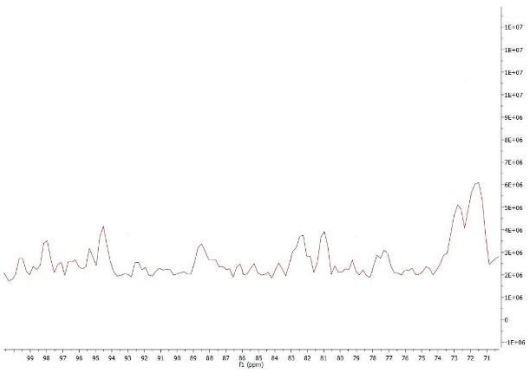

Figure 2b: 13C NMR Spectrum of Paspaloside

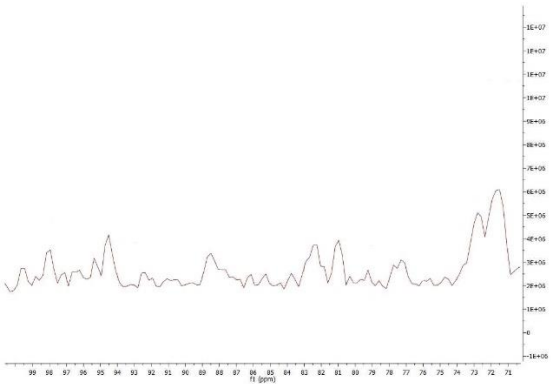

Figure 2c: 13C NMR Spectrum of Paspaloside

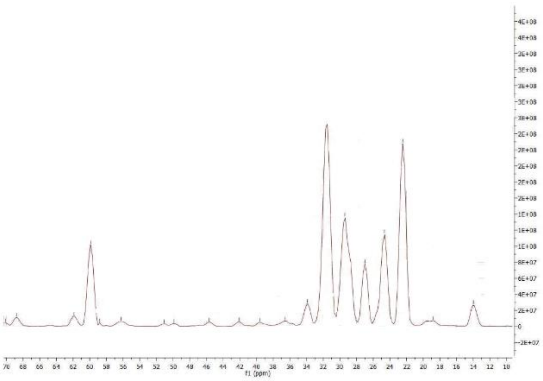

Figure 2d: 13C NMR Spectrum of Paspaloside

Table 3. ^{13}C NMR Spectral Data of Paspaloside (Figure 2a–2d)

δ (ppm)	Carbon Type	Assignment	Interpretation
18.2	CH_3	Cymarose C-6	6-deoxy sugar
35.6	CH	Cymarose C-2	Deoxy sugar framework
57.5	OCH_3	3-O-methyl	Diagnostic cymarose signal
60.5–62.5	CH_2	C-6 of hexoses	Glycosidic linkage
68.0–78.5	CH	Sugar ring carbons	Oxygenated carbons
96.0	C	Cymarose anomeric C-1	β-linked deoxy sugar
100.7–105.2	C	Anomeric carbons	β-glycosidic bonds
128.4, 129.6	C	Olefinic carbons	Steroidal nucleus
172.8–173.6	C=O	Carbonyl carbon	Ester/lactone function

The first spectrum (^{1}H NMR) displays proton resonances in the chemical shift range of 0–8 ppm, indicating the presence of different proton environments such as aliphatic and possibly aromatic or heteroatom-adjacent protons **[Table 4 & Table 5]**. The distribution and intensity of the peaks suggest chemically non-equivalent hydrogen atoms within the molecular framework, while the absence of signals beyond 9 ppm indicates the likely absence of aldehydic or strongly acidic protons. The spectrum was properly calibrated using an external reference, as indicated by the “EXTERNAL-ACC.K” notation [29].

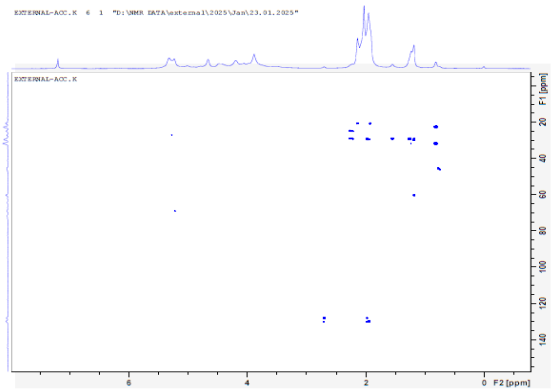

Figure 3: HSQC Spectrum of Paspaloside

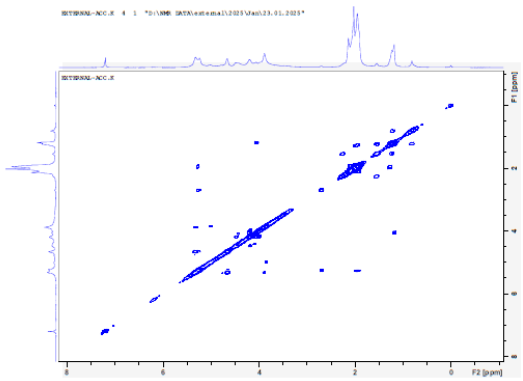

Figure 4: COSY Spectrum of Paspaloside

The second spectrum corresponds to the ^{13}C NMR, showing carbon resonances over a wide chemical shift range of approximately 20–140 ppm, which is characteristic of organic carbon skeletons. Peaks appearing in the downfield region (above ~100 ppm) can be attributed to sp^2-hybridized carbons such as aromatic or olefinic carbons, while signals in the upfield region (20–60 ppm) correspond to aliphatic carbons. The number and distribution of carbon signals indicate the presence of multiple chemically distinct carbon environments, supporting the proposed molecular structure. External referencing confirms accurate chemical shift assignment and spectral reliability [30].

Table 4. HSQC Correlation Summary (Figure 3)

Proton (δH ppm)	Carbon (δC ppm)	Correlation	Assignment
4.52	96.0	^{1}JCH	Cymarose H-1/C-1
4.60–4.90	100.7–105.2	^{1}JCH	Anomeric sugar carbons
3.55	57.5	^{1}JCH	O-methyl group
1.26	18.2	^{1}JCH	Cymarose CH_3

The third NMR spectrum, recorded under similar conditions, further supports the compound's structural consistency. The chemical shift range and signal pattern closely resemble those observed in the previous carbon spectrum, confirming reproducibility and structural stability. Minor variations in signal intensity may arise from experimental conditions or relaxation effects; however, the overall spectral features reinforce the presence of a stable organic framework with both aliphatic and unsaturated carbon environments. Together, these three NMR spectra provide strong evidence for the successful formation and structural integrity of the synthesized compound [31].

Table 5. COSY Correlation Summary (Figure 4)

Proton Pair	Correlation	Structural Meaning
H-1 ↔ H-2 (sugars)	Strong	Sugar ring continuity
H-2 ↔ H-3	Present	Glycosidic backbone
H-5 ↔ H-6	Observed	Hexopyranose structure
Cymarose CH_3 ↔ H-5	Weak	Deoxy sugar confirmation

Mass Spectral Analysis

The mass spectrum of Paspaloside exhibited a prominent molecular ion peak at m/z 1307, corresponding to the intact glycosidic molecule. Stepwise fragmentation peaks observed at m/z 1127, 947, 767, 587, 408, 270, 253, 210, 120, 105, and 163 indicated the sequential loss of sugar units, confirming the oligosaccharide nature of the compound **[Table 6]** [29].

Table 6. Mass Spectral Fragmentation Pattern

m/z	Fragment	Interpretation
1307	$[M]^+$	Molecular ion peak
1127	$[M – Hexose]^+$	Sugar loss
947	$[M – 2 Hexose]^+$	Oligosaccharide cleavage
767	$[M – 3 Hexose]^+$	Stepwise fragmentation
587	$[M – 4 Hexose]^+$	Confirms tetraglycoside
408	Aglycone	Steroidal nucleus
163	Cymarose	Deoxy sugar

180	Hexose	Glc/Gal/Man

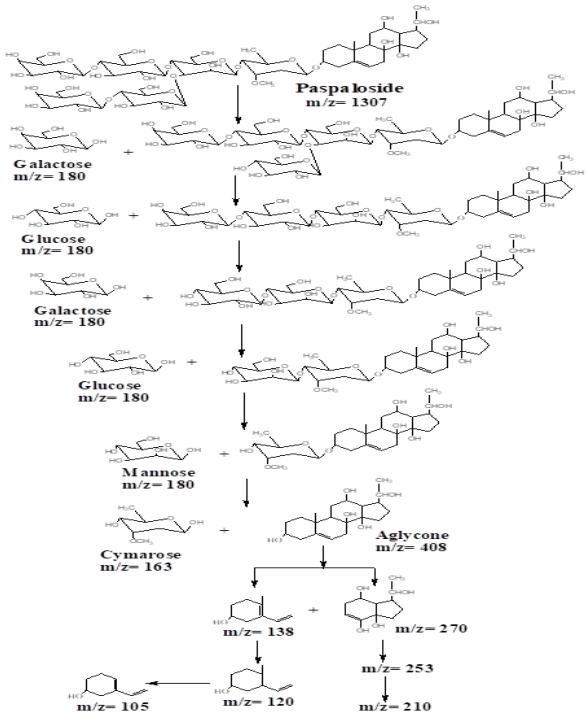

Mass Fragmentation of Paspaloside

The mass spectrum of Paspaloside exhibited a prominent molecular ion peak at m/z 1307, corresponding to the intact glycosidic molecule. Stepwise fragmentation indicated the sequential loss of its six sugar units. Diagnostic fragment ions at m/z 180 were consistent with the presence of hexose units (D-galactose, D-glucose, and D-mannose), while the fragment at m/z 163 was attributed to the cymarose residue. A characteristic aglycone fragment was observed at m/z 408, supporting a steroidal nucleus. The fragmentation pattern, showing the loss of multiple hexose residues, is fully consistent with a hexaglycosidic structure rather than a tetraglycoside. Diagnostic fragment ions at m/z 180 were consistent with the presence of hexose units (glucose, galactose, and mannose), while the fragment at m/z 163 was attributed to cymarose. A characteristic aglycone fragment was observed at m/z 408, supporting the presence of a steroidal nucleus. Additional low-mass fragments at m/z 270, 258, 210, 138, 120, and 105 further corroborated the sugar cleavage pattern and aglycone backbone. The fragmentation pathway is fully consistent with previously reported steroidal glycosides of a similar structural class [30].

Sugar Sequence and Linkage Analysis

The sugar sequence was deduced from combined NMR and mass spectral data. The large coupling constants of the anomeric protons confirmed β-linkages for all sugar residues. Acid hydrolysis followed by TLC analysis identified D-galactose, D-glucose, D-mannose, and cymarose as the constituent sugars [31].

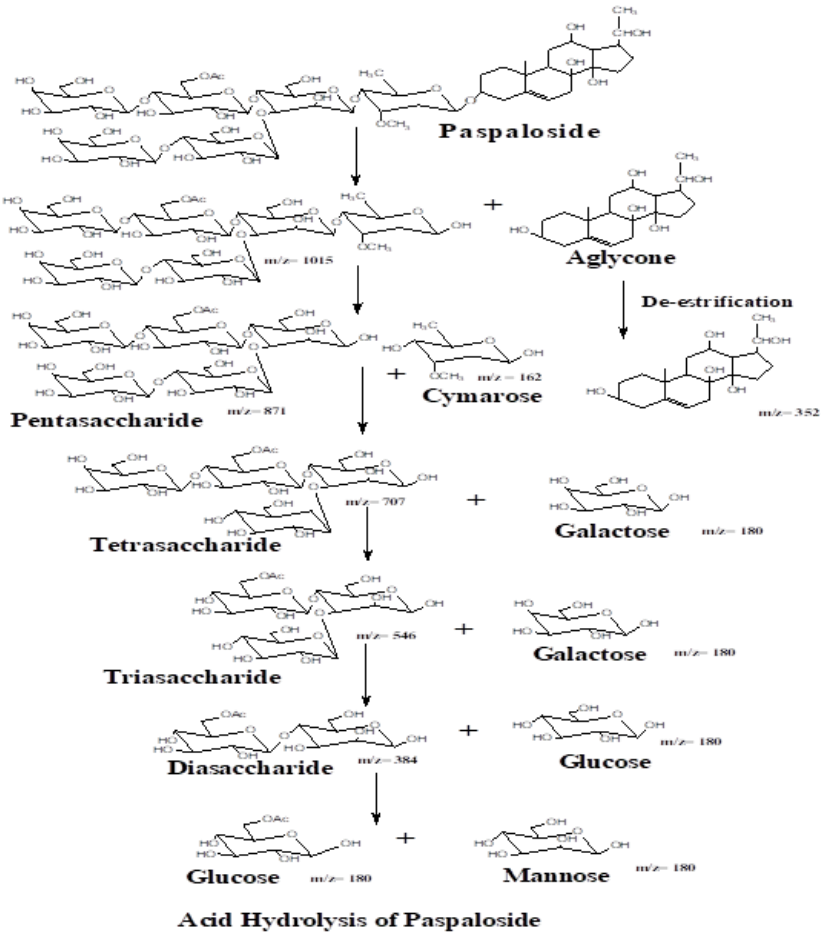

Table 7. Sugar Composition and Linkage Assignment

Sugar Unit	Configuration	Linkage	Evidence
Galactose (2)	β-D	(1→4)	C-4 downfield shift
Glucose (2)	β-D	(1→4)	Anomeric J = 7–8 Hz
Mannose (1)	β-D	(1→4)	C-6 deshielding
Cymarose (1)	β-D	Terminal	OCH_3 + CH_3 signals

The connectivity of the sugars was further supported by characteristic downfield shifts of glycosylated carbons observed in the 13C NMR spectrum. Based on these spectroscopic features, Paspaloside was established as a steroidal tetraglycoside with a branched oligosaccharide chain composed of β-linked galactose, glucose, mannose, and cymarose units attached to the aglycone moiety [32].

CONCLUSION

The present investigation led to the successful isolation and comprehensive structural elucidation of Paspaloside, a complex branched glycosidic compound from *Paspalum scrobiculatum* L. Detailed spectroscopic analyses, particularly extensive 1H and 13C NMR studies supported by mass spectrometry and acid hydrolysis, unambiguously established Paspaloside as a β-linked oligosaccharide glycoside composed of galactose, glucose, mannose, and a terminal cymarose unit attached to a steroidal aglycone. The presence of multiple β-anomeric proton signals, characteristic downfield shifts of glycosylated carbons, diagnostic cymarose resonances, and stepwise sugar fragmentation patterns in the mass spectrum collectively confirmed the sugar sequence, branching pattern, and overall molecular architecture. This study contributes valuable phytochemical knowledge to *P. scrobiculatum*, a nutritionally important but chemically underexplored millet crop, and enriches the growing database of structurally diverse natural glycosides. The well-defined structure of Paspaloside provides a reliable foundation for future investigations into its biosynthetic origin and potential biological activities. Overall, the findings highlight the importance of detailed spectroscopic approaches in the characterization of complex natural glycosides and underscore the phytochemical richness of edible plant resources.

REFERENCES:

1. Sabuz, A. A., Rana, M. R., Ahmed, T., Molla, M. M., Islam, N., Khan, H. H., ... & Shen, Q. (2023). Health-Promoting Potential of Millet: A Review. Separations, 10(2), 80. 10.3390/separations10020080
2. Shahi, S. (2019). “Avososе” Isolation and Structure Elucidation of Novel octasaccharide from Gaddi Sheep’s Milk. International Journal of Advanced Science and Technology, 27, 210 - 221. Retrieved from http://sersc.org/journals/index.php/IJAST/article/view/134
3. Anitha, S., Botha, R., Kane-Potaka, J., Givens, D. I., Rajendran, A., Tsusaka, T. W., & Bhandari, R. K. (2021). Can Millet Consumption Help Manage Hyperlipidemia and Obesity?: A Systematic Review and Meta-Analysis. Frontiers in nutrition, 8, 700778. https://doi.org/10.3389/fnut.2021.700778 .
4. Sadhukhan, A., & Debangshi, U. (2023). Millets in Meeting the Nutrition Security: A Review. Just Agriculture e-magazine, 3(5), 35-40. https://l1nq.com/dseuN
5. Tripathy, P., & Shahi, S. (2024). AI-Powered Mining of Nature's Chemical Library: Unveiling the Therapeutic Potential of Natural Products. Res. *J. Pharm*, *18*, 32-37. https://doi.org/10.36478/makrjp.2024.3.32.37.
6. Choudhari, M. K., Tiwari, R. K., Mishra, R. M., & Namdeo, K. N. (2018). Integrated nutrient management on growth, yield and economics of kodo millet (Paspalum scrobiculatum L.). Ann Plant Soil Res, 20(4), 405-408. https://sl1nk.com/lBxLF
7. Tripathy, P., Yadav, S. K., & Shahi, S. (2024). NANOMEDICINE: REVOLUTIONIZING HEALTHCARE THROUGH INNOVATION. *Bulletin of Pure & Applied Sciences-Zoology*, *43*. https://sl1nk.com/yT5z2
8. Amadou, I., Gounga, M. E., & Le, G. W. (2013). Millets: Nutritional composition, some health benefits and processing-A review. Emirates Journal of Food and Agriculture, 501-508. https://doi.org/10.9755/ejfa.v25i7.12045
9. Bunkar, D. S., Goyal, S. K., Meena, K. K., & Kamalvanshi, V. (2021). Nutritional, functional role of kodo millet and its processing: a review. International Journal of Current Microbiology and Applied Sciences, 10(01), 1972-1985. https://doi.org/10.20546/ijcmas.2021.1001.229
10. Praveen, K. V., & K, N. B. (2013). Economics analysis of minor millets in Bastar district of Chhattisgarh. African Journal of Agricultural Research, 8(39), 4928-4931. https://doi.org/10.5897/AJAR2012.2125
11. Shahi, S., Singh, H. K., Shukla, C. S., Deepak, D., & Singh, S. K. (2020). The Biological Utilization of Gaddi Sheep’s Milk Oligosaccharides. Journal of Critical Reviews, 7(15), 2061-2068.
12. Chandrakar, L., & Shahi, S. (2023). Millets and their Nutritional Value: A Review. Journal of Advanced Zoology, 44(S3), 1690-1697. https://l1nq.com/auPHE
13. Chandrasekara, A., & Shahidi, F. (2010). Content of insoluble bound phenolics in millets and their contribution to antioxidant capacity. Journal of agricultural and food chemistry, 58(11), 6706–6714. https://doi.org/10.1021/jf100868b
14. Bijalwan, V., Ali, U., Kesarwani, A. K., Yadav, K., & Mazumder, K. (2016). Hydroxycinnamic acid bound arabinoxylans from millet brans-structural features and antioxidant activity. International journal of biological macromolecules, 88, 296–305. https://doi.org/10.1016/j.ijbiomac.2016.03.069
15. Shahi, S., & Singh, S. K. (2022). Medicinal Plants in Chhattisgarh State. Journal of Pharmaceutical Negative Results, 647-653.
16. Shahi, S., & Singh, S. K. (2019). Biological importance of milk oligosaccharides isolated from Gaddi sheep's milk. EurAsian Journal of BioSciences, 13(2), 1245-1249.
17. Dey, S., Saxena, A., Kumar, Y., Maity, T., & Tarafdar, A. (2022). Understanding the antinutritional factors and bioactive compounds of kodo millet (Paspalum scrobiculatum) and little millet (Panicum sumatrense). Journal of Food Quality, 2022, 1-19. https://doi.org/10.1155/2022/1578448
18. Khare, P., Maurya, R., Bhatia, R., Mangal, P., Singh, J., Podili, K., ... & Kondepudi, K. K. (2020). Polyphenol rich extracts of finger millet and kodo millet ameliorate high fat diet-induced metabolic alterations. Food & function, 11(11), 9833-9847. https://doi.org/10.1039/d0fo01643h.
19. Goswami, D., Gupta, R. K., Mridula, D., Sharma, M., & Tyagi, S. K. (2015). Barnyard millet-based muffins: Physical, textural, and sensory properties. LWT-Food Science and Technology, 64(1), 374-380. https://doi.org/10.1016/j.lwt.2015.05.060
20. Shahi, S., & Singh, S. K. (2019). Biological importance of milk oligosaccharides isolated from Gaddi sheep's milk. EurAsian Journal of BioSciences, 13(2), 1245-1249.
21. Ceasar, S. A., & Ignacimuthu, S. (2010). Effects of cytokinins, carbohydrates and amino acids on induction and maturation of

somatic embryos in kodo millet (Paspalum scorbiculatum Linn.). Plant Cell, Tissue and Organ Culture (PCTOC), 102, 153-162. https://doi.org/10.1007/s11240-010-9716-6

22. Muragod, P. P., Muruli, N. V., Padeppagol, S., & Kattimani, A. (2019). Physico-chemical properties and nutritional factors of kodo millet. Int J Pure App Biosci, 7(1), 117-123. doi: http://dx.doi.org/10.18782/2320-7051.7297
23. Nagre, K., Singh, N., Ghoshal, C., Tandon, G., Iquebal, M. A., Nain, T., Bana, R. S., & Meena, A. (2023). Probing the potential of bioactive compounds of millets as an inhibitor for lifestyle diseases: molecular docking and simulation-based approach. Frontiers in nutrition, 10, 1228172. https://doi.org/10.3389/fnut.2023.122817233.
24. Neelam, Y., Kanchan, C., Alka, S., & Alka, G. (2013). Evaluation of hypoglycemic properties of kodo millet based food products in healthy subjects. IOSR J. Pharm, 3, 14-20. 35. https://sl1nk.com/qrruo
25. Srivastav, A., Shukla, M., Khare, N. K., & Deepak, D. (2025). 2-D NMR studies of geneoside, a novel pregnane pentaglycoside of 2-deoxy and 2, 6 dideoxy monosaccharides from ‘Wattakaka lanceolata’. *Natural Product Research*, *39*(8), 2187-2196. https://doi.org/10.1080/14786419.2023.2294476
26. García, V. P. (2011). Acid epimerization of 20-keto pregnane glycosides is determined by 2D-NMR spectroscopy. *Journal of Biomolecular NMR*, *50*(1), 91-97. https://doi.org/10.1007/s10858-011-9499-z
27. Palaniappan, A., Balasubramaniam, V. G., & Antony, U. (2017). Prebiotic potential of xylooligosaccharides derived from finger millet seed coat. *Food Biotechnology*, *31*(4), 264-280. https://doi.org/10.1080/08905436.2017.1369433
28. Rao, R. S. P., & Muralikrishna, G. (2007). Structural characteristics of water-soluble feruloyl arabinoxylans from rice (Oryza sativa) and ragi (finger millet, Eleusine coracana): Variations upon malting. *Food Chemistry*, *104*(3), 1160-1170. https://doi.org/10.1016/j.foodchem.2007.01.015
29. Veenashri, B. R., & Muralikrishna, G. (2011). In vitro anti-oxidant activity of xylo-oligosaccharides derived from cereal and millet brans–A comparative study. Food Chemistry, 126(3), 1475-1481. https://doi.org/10.1016/j.foodchem.2010.11.163
30. Palaniappan, A., Balasubramaniam, V. G., & Antony, U. (2017). Prebiotic potential of xylooligosaccharides derived from finger millet seed coat. Food Biotechnology, 31(4), 264-280. https://doi.org/10.1080/08905436.2017.1369433
31. Madhukumar, M. S., & Muralikrishna, G. (2010). Structural characterisation and determination of prebiotic activity of purified xylo-oligosaccharides obtained from Bengal gram husk (Cicer arietinum L.) and wheat bran (Triticum aestivum). *Food Chemistry*, *118*(2), 215-223. https://doi.org/10.1016/j.foodchem.2009.04.108
32. Rao, R. S. P., & Muralikrishna, G. (2007). Structural characteristics of water-soluble feruloyl arabinoxylans from rice (Oryza sativa) and ragi (finger millet, Eleusine coracana): Variations upon malting. Food Chemistry, 104(3), 1160-1170. https://doi.org/10.1016/j.foodchem.2007.01.015

